Influence of truncation angle on natural convection over a lower dome

Min-Seo Park*, Su-Yeon Park, Bum-Jin Chung†
Department of Nuclear Engineering, Kyung Hee University
1732 Deogyeong-daero Giheung-gu Yongin-si Gyeonggi-do 17104 (Republic of Korea)
bjchung@khu.ac.kr

***Keywords : i-SMR, dome, natural convection, truncation angle**

1. Introduction

In many Small Modular Reactors (SMRs), passive systems are adopted to cool the reactor core during accident conditions. In an accident, evaporated hot coolant released from the top of the reactor vessel (RV) to the containment vessel (CV), condenses along the containment wall. The condensed coolant accumulated at the bottom of the CV and it reintroduced to the RV through emergency recirculation valve (ERV) [1–3]. Since the ERV is located near the reactor core, the accumulated coolant can be exposed to high temperatures. This can lead to local boiling near the ERV entrance, potentially disturbing the reintroduction flow. In order to ensure the reintroduction of the condensate to the RV, the cooling capability of the lower dome becomes important. Therefore, the external natural convection heat transfer over the lower dome part of the CV governs the cooling capability of this region and plays a crucial role.

However, the external natural convection around the lower dome have been scarcely studied, only hemispherical (θ = 90°) or disk shape (θ = 0°) [4–7]. The geometry of a dome is characterized by the base diameter (D_b) and the truncation angle (θ), defined as the polar angle from the apex to the edge of the base disk as shown in Fig. 1.

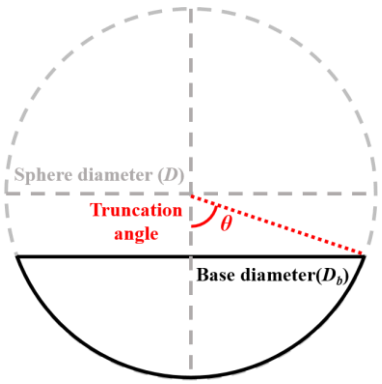

Fig. 1. Geometrical factors of the dome concept.

For a lower hemisphere (θ = 90°), natural convection heat transfer is generally stronger than that of a downward-facing horizontal plate [4]. At the central region of a curved surface, buoyancy has a tangential component along the surface, which accelerates the flow from the stagnation point, while the velocity increases toward the side. The presence of curvature allows boundary-layer growth, enhancing convective transport over the dome surface [5]. In contrast, a downward-facing plate/disk (θ = 0°) tends to exhibit thermal stratification near the center because buoyancy initially acts normal to the surface, resulting in weak acceleration and relatively low local heat transfer, while the plume mainly thins and accelerates the boundary layer near the trailing edge [6,7]. Therefore, the θ can be regarded as a key geometric parameter governing the balance between stratification-dominant and convective dominant.

Although natural convection over idealized geometries such as a hemisphere and a downward-facing disk has been investigated, studies on lower domes with intermediate truncation angles are lacking. In recently proposed SMR designs (e.g., VOYGR, i-SMR, and ACP100), however, the truncation angle of the lower dome ranges from 37° to 90°. Accordingly, the natural convection over the lower dome at the SMR scale was experimentally investigated for various Rayleigh numbers(Ra_{Db}) and θ.

2. Experimental setup

2.1 Methodology

We performed the mass experiment by adopting $CuSO_4$-H_2SO_4 electroplating system. As voltage applied, copper ions migrate towards the cathode and are reduced, resulting in a decrease in the concentration of copper ions around the cathode. The density difference caused by the difference in concentration at cathode generates buoyancy to analogy a natural convective heat transfer phenomenon. Therefore, transfer of copper ions from the anode to the cathode corresponds to natural convection heat transfer. This similarity allows the use of mass transfer experiments to simulate heat transfer phenomena based on the analogy concept as shown in Table 1.

To calculate the mass transfer coefficient (h_m) while overcoming the limitation of measuring the concentration of bulk fluid near the surface (C_b), the limiting current technique was adopted. In the electroplating system, the current initially increases and reaches a limiting current condition where all copper ions near the cathode are decreased. At this condition, the surface concentration is considered to be zero, which parallels the condition for constant temperature in heat transfer systems. Thus, the mass transfer coefficient (h_m) can be obtained only by determining the limiting current

density and bulk concentration as follow. Further details of the technique are explained in a previous study [8].

$$h_m = \frac{(1-t_{Cu^{2+}})I_{\lim}}{nFC_b} \quad (1)$$

Table 1. The governing parameters for heat and mass transfer systems [9]

Heat transfer		Mass transfer	
Nusselt number, (Nu_H)	$\frac{h_h D_b}{k}$	Sherwood number, (Sh_H)	$\frac{h_m D_b}{D_m}$
Prandtl number, (Pr)	$\frac{\nu}{\alpha}$	Schmidt number, (Sc)	$\frac{\nu}{D_m}$
Rayleigh number, (Ra_{Db})	$\frac{g\beta\Delta T D_b^3}{\alpha\nu}$	Rayleigh number, (Ra_{Db})	$\frac{gD_b^3}{D_m\nu}\frac{\Delta\rho}{\rho}$

2.2 Test matrix *and apparatus*

Table 2 indicates the test matrix for the experiments. Copper sulfate-sulfuric acid ($CuSO_4$-H_2SO_4) of 0.1 M and 1.5 M was used as working fluid corresponding to *Sc* of 2,094. The base diameter of dome was 0.025 m to 0.240 m, which corresponds to Ra_{Db} of 2.39×10^8 to 2.39×10^{12}, respectively. Among the test cases, the largest case (Ra_{Db} = 2.39×10^{12}) was designed to represent the geometric scale of the lower dome in the i-SMR. The truncation angles of domes were varied from 0° to 90° as shown in Fig. 2.

Table 2. Test matrix.

Sc (*Pr*)	Ra_{Db}	D_b (m)	Truncation angle, θ (°)
2,094	2.63×10^9	0.025	0, 10, 20, 30, 50, 70, 90
	1.08×10^{10}	0.040	
	1.68×10^{11}	0.100	
	2.39×10^{12}	0.240	

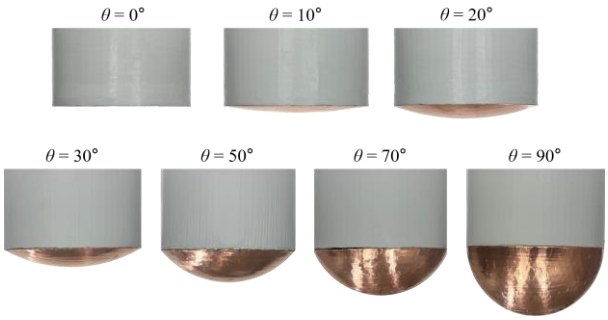

Fig. 2. Copper cathode apparatus for the dome of Ra_{Db} = 2.39×10^{12}.

Figure 3 illustrates the schematic image of the experimental setup. Cathode copper dome was placed at the center of an acrylic tank. The base part of the cathode dome was connected to an insulated cylinder to prevent the flow along the dome from intruding into the base surface. Four rectangular anodes located at each sides of the acrylic tank walls to ensure stable electrical current. The acrylic tank is filled with a $CuSO_4$-H_2SO_4 solution. Power is supplied through a power source (Vüpower K1810), and current is measured and recorded using a DAQ (NI 9227).

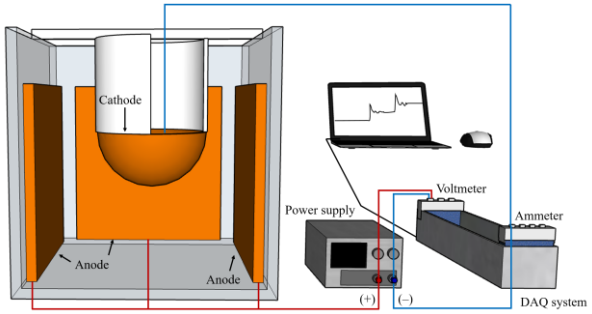

Fig. 3. Electric circuit and experimental apparatus.

3. Result and discussion

3.1 Data validation

Figure 4 demonstrates good agreement between the present experimental results for the dome with θ = 90° (hemispherical dome) and the existing natural convection heat transfer correlation for the lower part of a sphere [10]. The existing correlation covers a range up to $Gr_D \approx 10^9$, where the heat transfer can be represented by a single correlation [10]. The line indicates the existing correlations, and the symbols show the experimental cases for the dome with θ = 90°, respectively. To ensure experimental accuracy, all cases were repeated three times using two independent apparatuses, resulting in a total of six measurements for each condition. The average deviation among the six repeated experiments was 2.6 %.

The experimental results well matched with existing correlations: the average relative error with the correlation was within 5%.

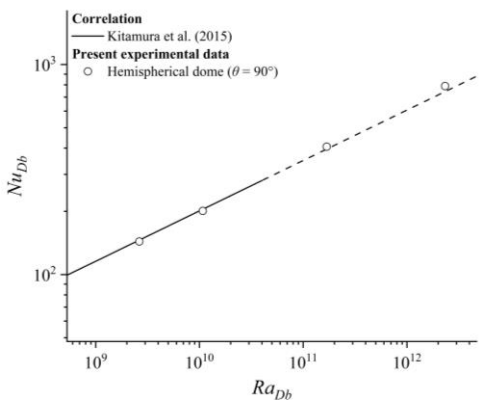

Fig. 4. The overall Nu_{Db} of the dome for θ = 90° with existing correlations.

3.2 Average Nu_{Db} according to truncation angle (θ)

Figure 5 presents the average Nu_{Db} of the dome for the entire experimental cases. For the entire Ra_{Db} conditions, Nu_{Db} increases as the truncation angle (θ) increases. The most significant variation in Nu_{Db} with respect to θ was observed in the range of $0° \leq \theta \leq 30°$. In contrast, the Nu_{Db} for domes with $\theta \geq 50°$ were nearly identical, showing a maximum deviation of only 3.3%.

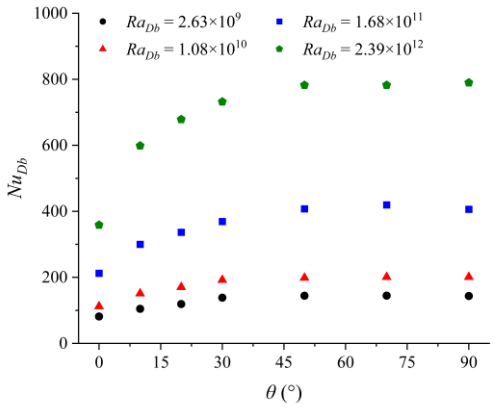

Fig. 5. The overall Nu_{Db} of the dome.

Figure 6 shows the Nu_{Db} values of domes at the same Ra_{Db}, presented as the ratio to the Nu_{Db} value of the θ = 90° dome. In the all cases, the $Nu_{Db}/Nu_{Db,\theta=90°}$ remains constant for each θ, regardless of Ra_{Db}.

For $0° \leq \theta \leq 30°$, the Nu_{Db} of the dome decreases as θ decreases. Compared with $\theta = 90°$ case, the average Nu_{Db} reduction was 47.5% at $\theta = 0°$ and 6.1% at $\theta = 30°$. With small truncation angle, the tangential buoyancy component over the dome decreases. It results in weakens the overall driving force of the flow. A lower driving promotes the thermal stratification, which in turn decreases heat transfer. The tangential buoyancy component over the dome increases as the truncation angle of the dome increases, thereby increasing the driving force. For $\theta \geq 50°$, the heat transfer shows little difference compared to the $\theta = 90°$ case, with a maximum deviation of only 3.3%. In the other words, within the range of $\theta \geq 50°$, the proportion of the surface where spontaneous buoyancy acceleration is possible remains sufficiently large. As a result, the overall driving force is maintained at a value comparable to that of the θ = 90° dome, and the heat transfer also remains nearly constant.

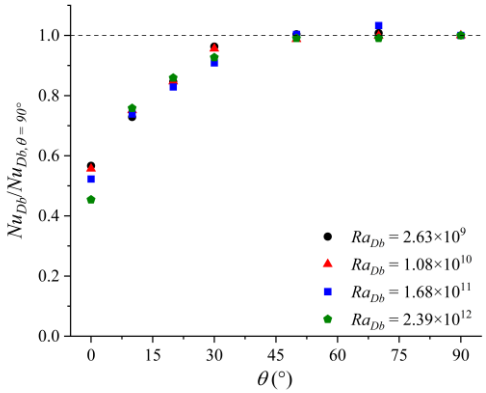

Fig. 6. Nu_{Db} ratio between truncated dome and $\theta = 90°$ dome.

3.3 Correlation fitting for truncated domes

The dome has a continuously varying surface inclination along a single curved surface. Therefore, it is difficult to represent the heat transfer characteristics using a single inclination angle, unlike a flat plate. Therefore, the truncation angle (θ) was introduced as a representative geometric parameter, and a heat transfer correlation was obtained as:

$$Nu_{Db} = 0.586 Ra_{Db}^{0.253}(1-0.579\ (1-\sin\theta)^{3.685}) \quad (2)$$

The basic form of the correlation was derived with reference to a basic hemispherical form of Nu_D ($Nu_D = C_1 + C_2\, Ra_D^{n}$) and a multiplier to correct the influence of truncation angle, $f(\theta)$, since no significant difference in the truncation-angle effect with respect to Ra_{Db} was observed.

Figure 8 presents the deviation between the experimental data and the values calculated using the fitted correlation. The relative error between the correlation and the experimental results was within a maximum of 13.1%, with an average error of 3.2%, indicating that the proposed correlation predicts the overall heat transfer with good accuracy.

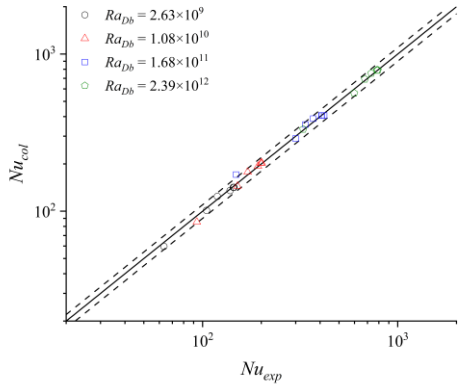

Fig. 8. Comparison of experimental results with calculated results by the fitted correlation.

4. Conclusion

This study experimentally investigated natural convection over lower domes with various truncation angle and Rayleigh numbers, focusing on the influence of the truncation angle (θ). For the entire Ra_{Db} conditions, the average Nu_{Db} increased with increasing θ. The most pronounced variation was observed in the range of $0° \leq \theta \leq 30°$, where Nu_{Db} decreased significantly as θ decreased. This reduction is attributed to the decrease in the tangential buoyancy component near the trailing edge, which weakens the overall driving force of the flow.

In contrast, for $\theta \geq 50°$, the heat transfer showed little dependence on θ, indicating that a sufficiently large portion of the dome surface can sustain buoyancy-driven acceleration and maintain a comparable global flow strength. Additionally, a heat transfer correlation was proposed with consideration of θ.

This work provides experimental data on external natural convection over lower domes with various θ at the SMR scale. The results contribute to evaluating thermal condition of coolant into ERV, thereby supporting safety analysis of passive containment cooling systems in SMRs. In future work, PIV experiments will be conducted to analyze the corresponding flow characteristics.

ACKNOWLEDGEMENT

This work was supported by the Innovative Small Modular Reactor Development Agency grant funded by Korea Government Ministry of Climate, Energy and Environment (MCEE) (No. RS-2024-00404240).

REFERENCES

[1] H. O. Kang, Light water SMR development status in Korea, Nuclear Engineering Design, Vol. 419, 2024
[2] C. H. Song, J. Song, S. J. Kim, Evaluation of accident mitigation capability of passive core and containment cooling systems of i-SMR under representative LOCA and non-LOCA conditions, Nuclear Engineering Technology, Vol. 57, 2025.
[3] S. G. Lim, H. S. Nam, D. H. Lee, S. W. Lee, Design Characteristics of Nuclear Steam Supply System and Passive Safety System for Innovative Small Modular Reactor (i-SMR), Nuclear Engineering Technology, Vol. 57, 2025
[4] F. J. Higuera, A. Linan, Pressure gradient effect in natural convection boundary layer, Physics of Fluids A: Fluid Dynamics, Vol. 5, 1993.
[5] S. Acharaya, Natural convection heat transfer from upward, downward, and sideward solid/hollow hemispheres, Journal of Thermophysics and Heat Transfer, Vol. 36, pp. 141–153, 2022.
[6] F. Restrepo, The effect of edge conditions on natural convection from a horizontal plate, International Journal of Heat and Mass Transfer, Vol. 17, pp. 135–142, 1974.
[7] M. K. Friedrich, D. Angirasa, The interaction between stable thermal stratification and convection under a heated horizontal surface facing downward, International journal of non-linear mechanics, Vol. 36, pp. 719–729, 2001.
[8] H.K. Park, B.J. Chung, Mass transfer experiments for the heat load during in-vessel retention of Core melt, Nuclear Engineering and Technology, Vol. 48, pp. 906–914, 2016.
[9] A. Bejan, Convection Heat Transfer, 4th ed., Wiley, New York, 2013
[10] K. Kitamura, A. Mitsuishi, T. Suzuki, T. Misumi, Fluid flow and heat transfer of high-Rayleigh-number natural convection around heated spheres, International Journal of Heat and Mass Transfer, Vol. 86, pp. 149–157, 2015.